

# The Thioredoxin Reductase Inhibitor Auranofin Suppresses Pulmonary Metastasis of Osteosarcoma, But Not Local Progression

HIDEYUKI KINOSHITA<sup>1</sup>, OSAMU SHIMOZATO<sup>2</sup>, TAKESHI ISHII<sup>1</sup>, HIROTO KAMODA<sup>1</sup>, YOKO HAGIWARA<sup>1</sup>, TOSHINORI TSUKANISHI<sup>1</sup>, SEIJI OHTORI<sup>3</sup> and TSUKASA YONEMOTO<sup>1</sup>

<sup>1</sup>Department of Orthopedic Surgery, Chiba Cancer Center, Chiba, Japan;

<sup>2</sup>Laboratory of Oncogenomics, Chiba Cancer Center Research Institute, Chiba, Japan;

<sup>3</sup>Department of Orthopedic Surgery, Graduate School of Medicine, Chiba University, Chiba, Japan

**Abstract.** *Background/Aim:* Auranofin (AUR), a thioredoxin reductase (TXNRD) inhibitor, shows anticancer activity against several cancers. This study investigated the effects of AUR on the local progression and pulmonary metastasis of osteosarcoma (OS). *Materials and Methods:* Publicly available expression cohorts were analysed to study the relationship between TXNRD-2 expression and the survival of patients with OS. The murine OS cell line LM8 was stimulated with AUR. Cell viability, apoptosis-related protein levels, caspase activity, and wound healing were analysed. Tumor progression and pulmonary metastasis were investigated in C3H mice implanted with LM8 cells. *Results:* High-level expression of TXNRD-2 represented a negative prognostic factor for metastasis and overall survival in patients with OS. AUR induced apoptosis of OS cells via the oxidative stress-MAPK-Caspase 3 pathway, and suppressed the migration of OS cells. AUR inhibited the pulmonary metastasis of OS, but not local progression. *Conclusion:* AUR represents a potential therapeutic drug for suppressing pulmonary metastasis of OS.

Osteosarcoma (OS) is a relatively rare malignant tumor with a high incidence in the adolescent and young adult population, and is associated with poor survival. Treatment of OS includes surgery and perioperative chemotherapies (1). Standard chemotherapy for pediatric patients involves the use of doxorubicin, cisplatin, and high-dose methotrexate. However, the five-year survival probability for OS is poor, and it is worse

for patients with pulmonary metastases. Chemotherapies used at present include conventional cytotoxic agents with strong side effects; therefore, the development of novel therapeutic agents is desirable. The oxidation-reduction (redox) system is an essential regulator of various metabolic functions of the cell. Thioredoxin (TXN), a key molecule in the redox system, plays an active role in scavenging reactive oxygen species (ROS), which are associated with the development of several diseases, including cancers and sarcomas (2, 3). ROS has been shown to activate mitogen-activated protein kinases (MAPKs), such as p38 and c-Jun N-terminal kinase (JNK), and induce apoptosis in cancer cells (4). TXN reductases (TXNRDs) are enzymes that catalyse the reduction of TXN and regulate TXN activity. Members of the TXNRD family comprise three isoforms including cytosolic TXNRD-1, mitochondrial TXNRD-2, and TXNRD-3. TXNRD-2 has been reported to be often overexpressed in cancer cells thereby conferring resistance to apoptosis (5); TXNRDs represent therapeutic targets of several cancers (6). Auranofin (AUR) is an anti-rheumatic drug approved by the US Food and Drug Administration (FDA) that functions as a TXNRD inhibitor and has anticancer properties against several cancers (7, 8). The effect of AUR alone on local progression and pulmonary metastases of OS has not been reported in previous studies. Therefore, we investigated the effects of AUR on local progression and pulmonary metastasis of OS *in vitro* and *in vivo*.

## Materials and Methods

**Bioinformatics.** We evaluated the association of TXNRD-2 gene (ILMN\_1653904) expression with the outcomes of patients with OS using public microarray data (GSE42352). TXNRD-2 gene expression data were downloaded from the R2 microarray analysis and visualization platform, and the R2-based application was used to draw Kaplan–Meier survival curves. The best cut-off in survival analyses was selected as the expression value where the statistic log-rank for the separation of survival curves reached its higher level.

*Correspondence to:* Hideyuki Kinoshita, Department of Orthopedic Surgery, Chiba Cancer Center, 666-2 Nitonacho, Chuo-ku, Chiba 260-8717, Japan. Tel: +81 432645431, Fax: +81 432628680, e-mail: kinoshi1783@yahoo.co.jp

**Key Words:** Osteosarcoma, thioredoxin reductase, auranofin, pulmonary metastasis.

**Antibodies and reagents.** Antibodies and reagents were obtained from the following commercial sources: AUR, Santa Cruz Biotechnology (Santa Cruz, CA, USA); N-Acetyl-L-cysteine (NAC), Sigma-Aldrich (St. Louis, MO, USA); carbobenzoxy-valyl-alanyl-aspartyl-[O-methyl]-fluoromethylketone (Z-VAD-FMK), Adooq bioscience (Tokyo, Japan); MEM, Sigma-Aldrich; radioimmunoprecipitation acid (RIPA) lysis buffer, Santa Cruz Biotechnology; anti-p38 MAPK (#9212), anti-JNK MAPK (#9252), anti-phospho-p38 MAPK (Thr180/Tyr182) (#9211), anti-phospho-JNK MAPK (Thr183/ Tyr185) (#9251), and cleaved caspase-3 (Asp175) (#9661) were obtained from Cell Signaling Technology (Danvers, MA, USA); horseradish peroxidase-conjugated secondary antibodies and polyvinylidene difluoride (PVDF) western blotting membrane, GE Healthcare (Tokyo, Japan).

**Cell culture.** The LM8 cell line (RRID: CVCL\_6669) was obtained from RIKEN BioResource Center (Ibaraki, Japan). Cell lines were maintained in MEM supplemented with 10% fetal bovine serum (FBS) and 100 mg/ml penicillin/streptomycin in a humidified 5% CO<sub>2</sub> atmosphere at 37°C.

**Cell viability assay.** LM-8 cells were seeded at a concentration of 1×10<sup>6</sup> cells/ml in a 96-well plate and stimulated with AUR (1.25, 2.5, 5, 10, and 20 μM) or dimethyl sulfoxide (DMSO) for 12 and 24 h. Subsequently, 3-(4,5-dimethylthiazol-2-yl)-2,5-diphenyltetrazolium bromide solution (Cayman Chemical, Ann Arbor, MI, USA) was added at a volume equivalent to 10% of the culture volume under sterile conditions, and incubated for 4 h in a 5% CO<sub>2</sub> incubator at 37°C. After incubation, a crystal-dissolving solution was added to the cultures followed incubation for 4-18 h in a CO<sub>2</sub> incubator at 37°C. The absorbance of each sample at 570 nm was measured using a microplate reader (Multiskan sky, Thermo science, Tokyo, Japan). Cell viability (%) was calculated based on the following equation: (Experimental group absorbance value/Control group absorbance value) ×100.

**IncuCyte® cell proliferation assay.** Cell proliferation was monitored for 96 h using the IncuCyte® ZOOM system (Essen Bioscience, Ann Arbor, MI, USA), which uses an automated incubator method for monitoring live cells. Growth curves were generated using the algorithm in the ZOOM software by using data points acquired during six-hour-interval imaging. All samples were plated in quadruplicate.

**Immunoblotting.** All wash buffers and extraction buffers contained a protease inhibitor cocktail (Roche, Tokyo, Japan), NaF (1 M), PhosSTOP phosphatase inhibitor (Roche), and Na<sub>3</sub>VO<sub>4</sub> (50 μM). Cell extracts were separated using sodium dodecyl sulphate-polyacrylamide gel electrophoresis and electroblotted onto PVDF membranes. After blocking with 2% bovine serum albumin in TBS-T [150 mM NaCl, 50 mM Tris HCl (pH 8.0), and 0.05% Tween-20], the membranes were probed with antibodies. The antibody-antigen complexes were detected using an enhanced chemiluminescence system (GE Healthcare).

**Caspase assay.** Cells stimulated with DMSO or AUR were lysed using the RIPA lysis buffer without protease inhibitor. A substrate solution was prepared, which was mixed with phosphate-buffered saline (PBS), 2× Reaction Buffer (MBL, Tokyo, Japan), and caspase-3 substrate VII, Fluorogenic (Calbiochem, Darmstadt, Germany). The supernatant of the cells was mixed with the substrate solution in a 96-well plate. The plates were incubated at 37°C for 2 h in the dark, and the absorbance was measured using a microplate reader (Multiskan sky, Thermo science, Tokyo, Japan).

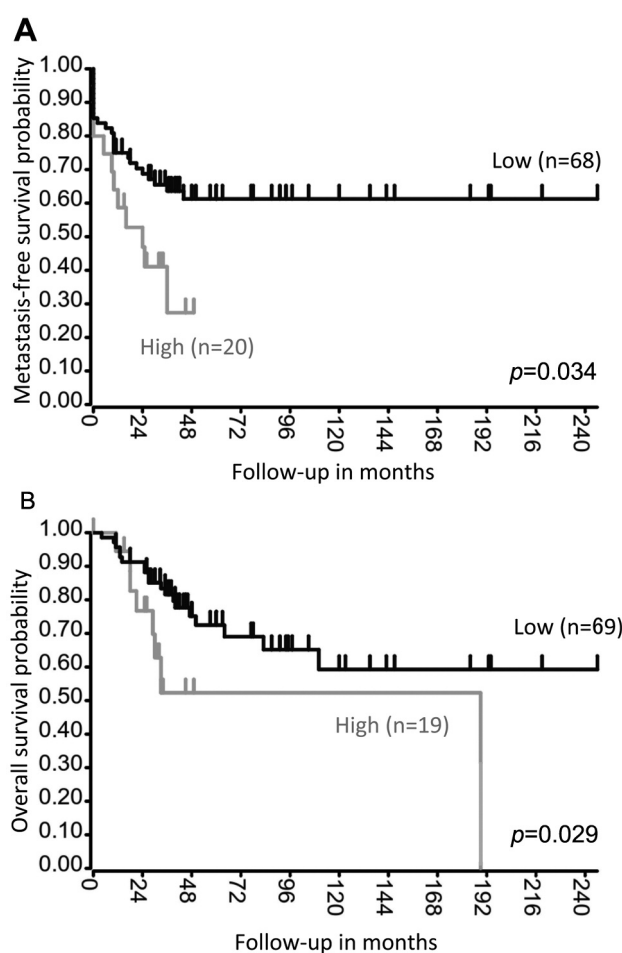


Figure 1. High-level expression of TXNRD-2 represents a negative prognostic factor for metastasis-free (A) and overall survival (B) in patients with osteosarcoma. Kaplan-Meier analysis using published array data from two independent sets of tumors [R2: Genomics Analysis and Visualization Platform (<http://r2.amc.nl>)]. TXNRD-2: Thioredoxin reductase-2.

**Wound healing assay.** Cells were seeded in 6-well plates and cultured till a confluent monolayer was obtained. A wound was created in the cell monolayer by scratching the plate using a sterile pipette tip, and the cells were washed using PBS. Pre-treatment using 10 μg/ml of Mitomycin C (Abcam, Tokyo, Japan) was performed at 37°C for 1 h to inhibit cell proliferation. Next, LM8 cells were incubated with DMSO or AUR (1 μM) in the presence of 10% FBS for 24 h. Cells were photographed at ×100 magnification at 0, 12, and 24 h after incubation. The distance migrated by the cells was measured between the two boundaries of the acellular area. The results of the different treatment groups were expressed as a ratio to the original distance.

**Animal studies.** Female five-week-old C3H/HeSlc mice were obtained from Japan SLC (Shizuoka, Japan). The mice were maintained at a constant temperature (22±2°C) and humidity (50±10%), with a 12h light/12h dark cycle. All animal experiments were approved by the Institutional Animal Care and Use Committee of Chiba Cancer Center,

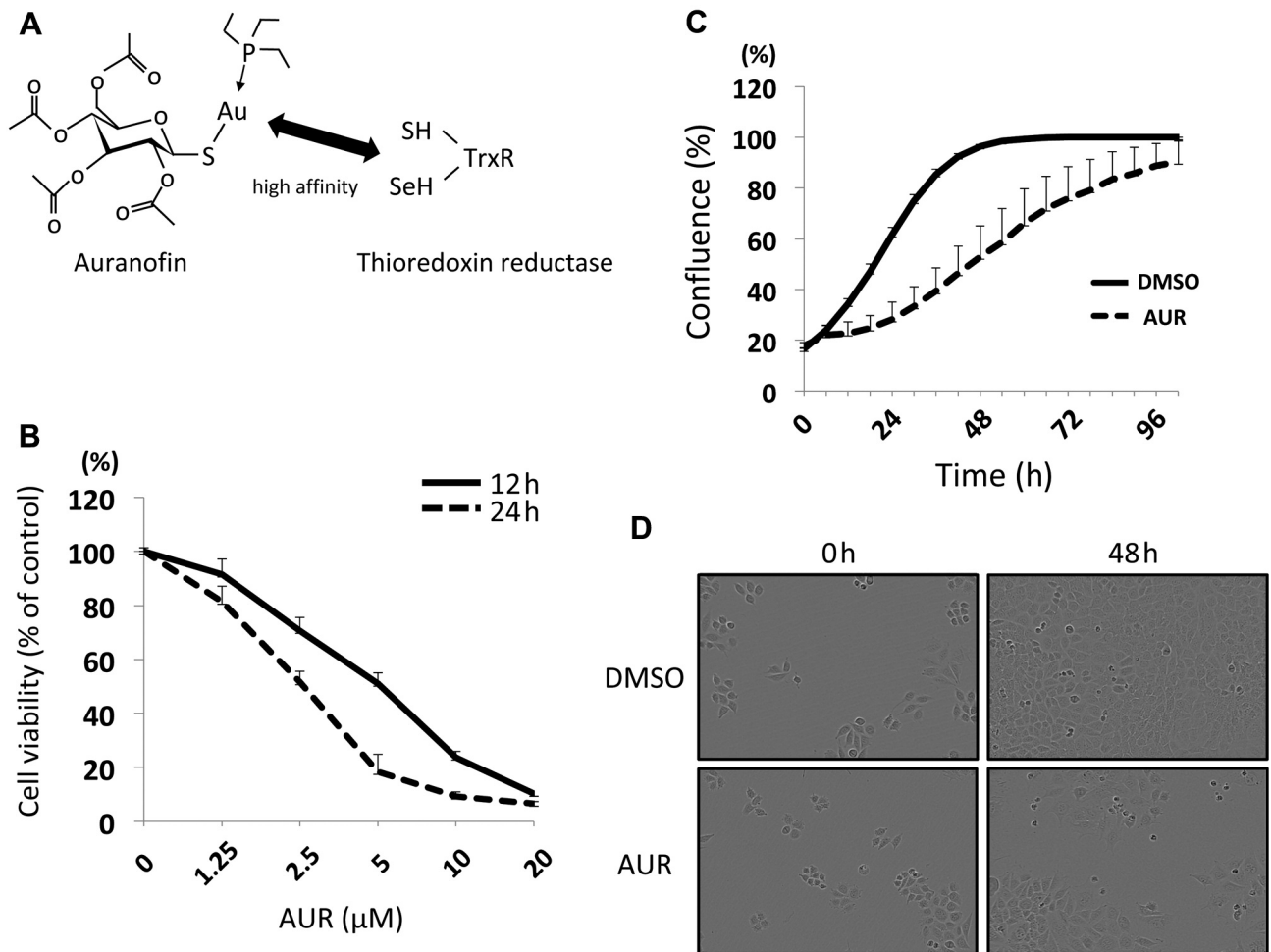


Figure 2. The effect of AUR on LM8 cell proliferation. (A) Schematic diagram of the interaction between AUR and thioredoxin reductase. (B) AUR induced the death of osteosarcoma cells in a dose- and time-dependent manner. (C) Low-dose AUR ( $0.2 \mu\text{M}$ ) inhibited the growth of LM8 cells in a cell proliferation assay. (D) Proliferation state of LM8 cells at 0 and 48 h. AUR: Auranofin.

Chiba, Japan, and were conducted in accordance with institutional guidelines. On day 0,  $1 \times 10^7$  LM8 cells in  $300 \mu\text{l}$  PBS were injected subcutaneously into the back of syngeneic C3H/HeSlc mice (12 mice). The growth of primary tumors to a measurable size (measured using a calliper and determined as  $\text{length} \times \text{width}^2/2$ ) was allowed to proceed for 7 d prior to treatment. Mice were then assigned to two groups of 6 mice with a similar distribution of tumor sizes. The mice were treated with either  $200 \mu\text{l}$  vehicle control (40% polyethylene glycol 300+60% sterile PBS) or  $10 \text{ mg/kg}$  AUR. Injections were administered when palpable tumors ( $100\text{--}150 \text{ mm}^3$ ) were observed, and were provided intraperitoneally every day till the end of the study. Tumor size measurements and animal weights were recorded once a week in a non-blinded manner. On day 35, the mice were euthanized under anaesthesia, and the tumors were resected for tumor weight measurement. Lung samples were harvested for further examination. The number of lung metastases was determined by counting the number of metastatic nodules on the lung surface. The lungs were then fixed with formalin and embedded in paraffin. Hematoxylin and eosin staining was performed to detect the lung metastasis.

**Statistical analysis.** Experimental data are expressed as the mean  $\pm$  standard deviation. Significant differences between mean values were calculated using Student's *t*-test; a value of  $p < 0.05$  was considered significant.

## Results

*High-level expression of TXNRD-2 was a negative prognostic factor for metastasis and overall survival in patients with OS.* Using publicly available expression cohorts, we analysed the expression levels of TXNRD-2 and their correlation to metastasis-free and overall survival in patients with OS (Figure 1A and B). High expression of TXNRD-2 correlated to poor metastasis-free and overall survival in the expression cohorts analysed, suggesting that TXNRD-2 may represent a therapeutic target associated with the progression and metastasis of OS.

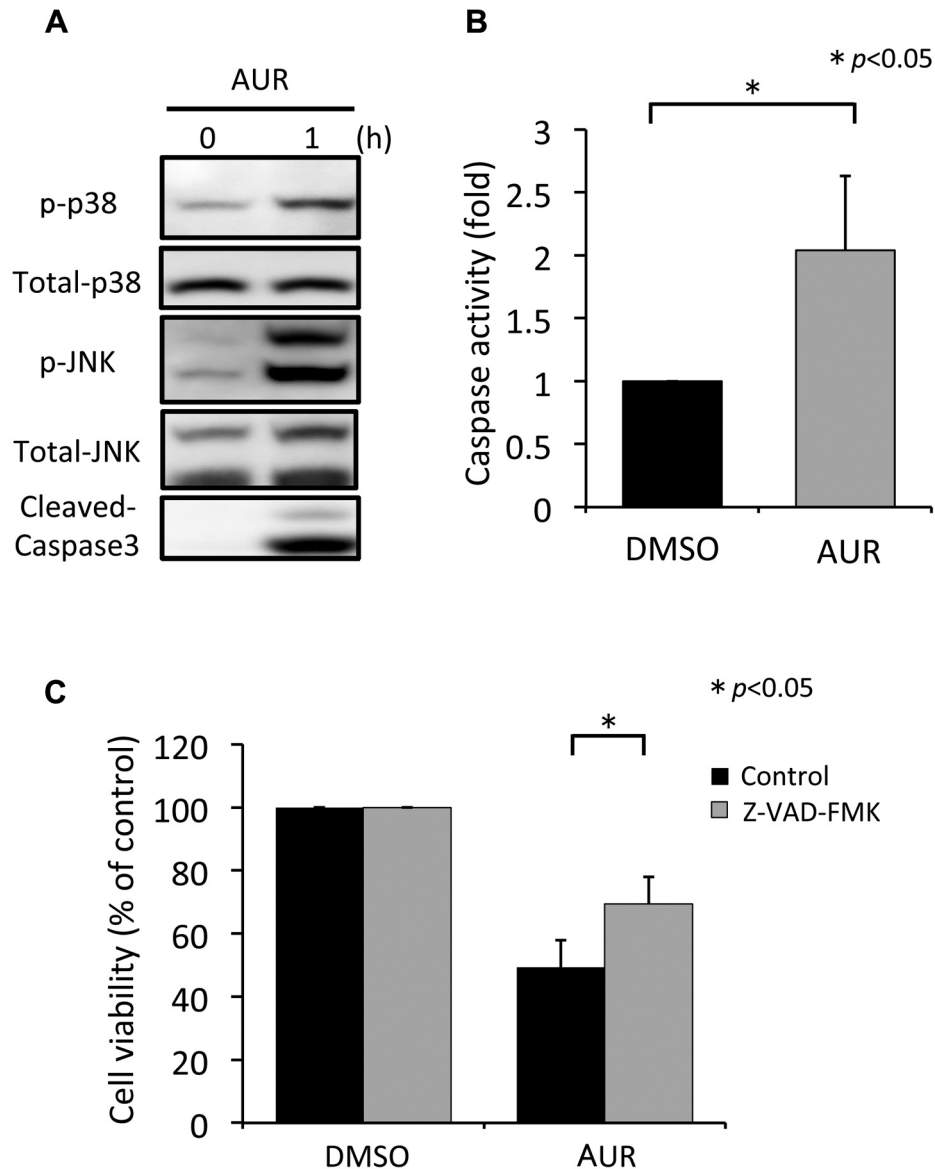


Figure 3. AUR induced apoptosis of OS cells via the MAPK-Caspase 3 pathway. (A) AUR (20 μM) induced the phosphorylation and activation of p38, JNK, and the caspase 3 cleavage in LM8 cells. (B) Caspase assays indicated AUR treatment (10 μM) induced two-fold caspase activity compared to that in the control. \* $p < 0.05$  ( $n = 3$ ). (C) Z-VAD-FMK, a pan-caspase inhibitor, significantly reversed the death of LM8 cells induced via AUR treatment (2 μM) \* $p < 0.05$  ( $n = 3$ ). AUR: Auranofoin; JNK: c-Jun N-terminal kinase; Z-VAD-FMK: carbobenzoxy-valyl-alanyl-aspartyl-[O-methyl]-fluoromethylketone.

The TXNRD inhibitor AUR induced apoptosis of OS cells via the oxidative stress-MAPK-Caspase 3 pathway. AUR is a gold-phosphine thiolate small molecule (Figure 2A). AUR is known to inhibit TXNRDs, such as TXNRD-1 and TXNRD-2, owing to the high affinity of gold for thiol and selenol nucleophiles present in TXNRDs (9). First, we evaluated the effect of AUR on LM8 cell proliferation. AUR induced the death of LM8 cells in a dose- and time-dependent manner (Figure 2B). Furthermore, low-dose AUR inhibited the growth of LM8 cells

as shown by a cell proliferation assay (Figure 2C and D). Western blotting analysis showed that AUR induced the phosphorylation and activation of p38, JNK, and caspase 3 cleavage, suggesting the induction of apoptosis in LM8 cells (Figure 3A). Caspase assays indicated the AUR induced two-fold caspase activity compared to that of the control (Figure 3B). Furthermore, Z-VAD-FMK, a pan-caspase inhibitor, significantly reversed AUR-induced death of LM8 cells (Figure 3C). NAC, an antioxidant and precursor of glutathione, reduced

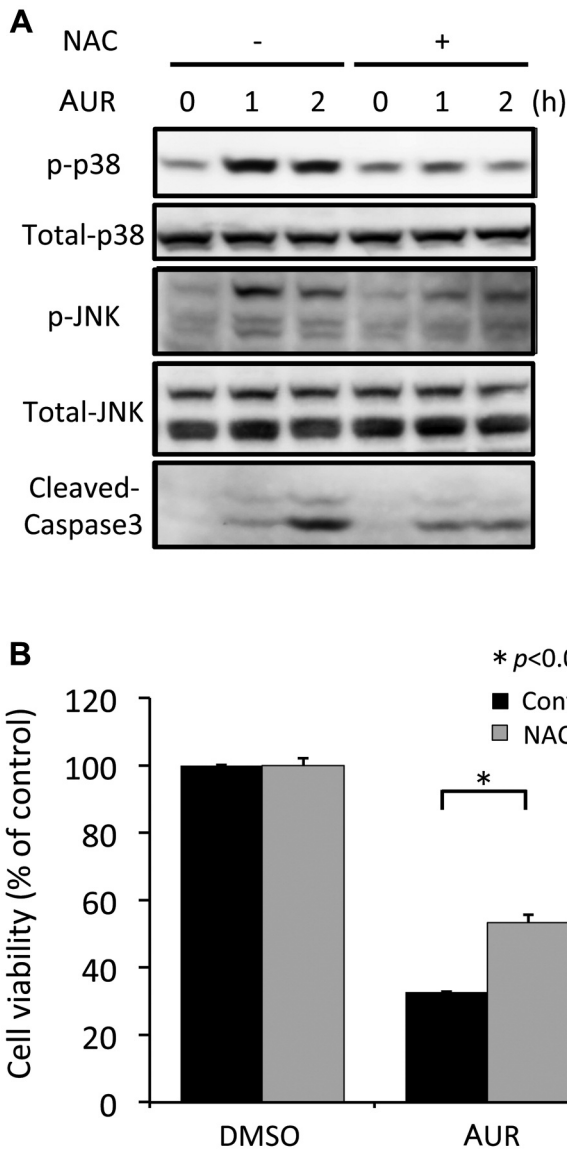


Figure 4. AUR induced apoptosis of OS cells via the oxidative stress-MAPK-Caspase 3 pathway. (A) Pre-treatment of cells with 1 mM NAC, an antioxidant, for 1 h reduced the activation of mitogen-activated protein kinases and cleavage of caspase-3 induced by AUR (20  $\mu$ M). (B) NAC (1 mM) significantly inhibited the death of LM-8 cells induced by AUR (2  $\mu$ M). \* $p$ <0.05 (n=3). NAC: N-Acetyl-L-cysteine; AUR: auranofin.

the activation of MAPK proteins and AUR-induced cleavage of caspase-3 (Figure 4A). Furthermore, NAC significantly inhibited AUR-induced death of LM-8 cells (Figure 4B), suggesting that AUR might have induced cell death via the oxidative stress-MAPK-Caspase 3 pathway.

*AUR suppressed the migration of OS cells.* We investigated whether AUR could inhibit the migration of LM8 cells via

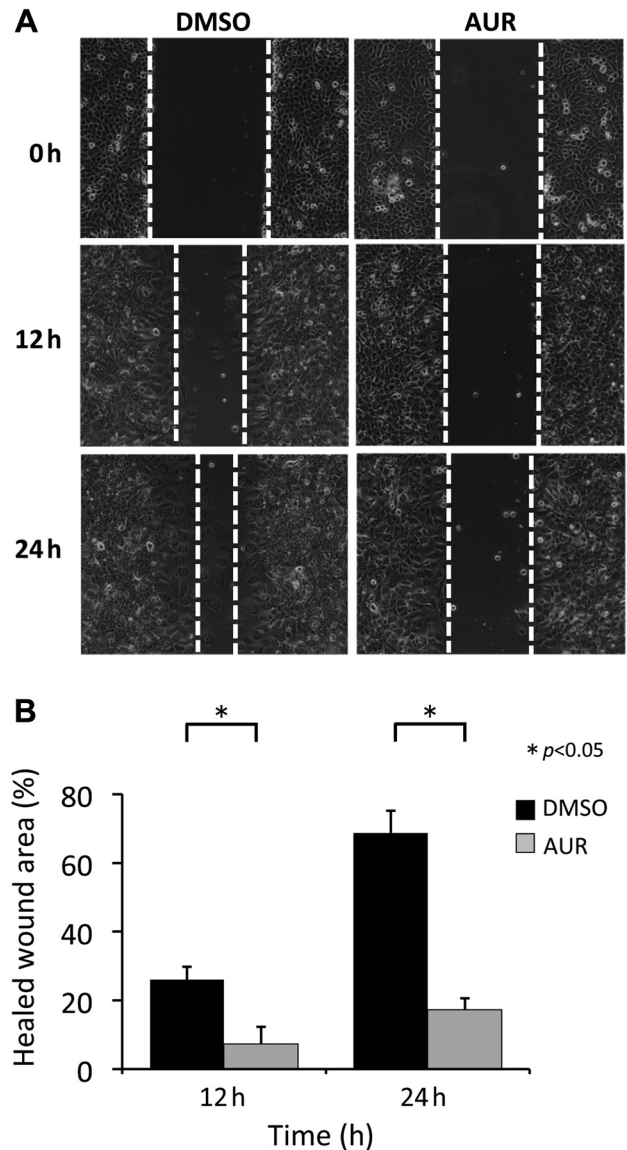
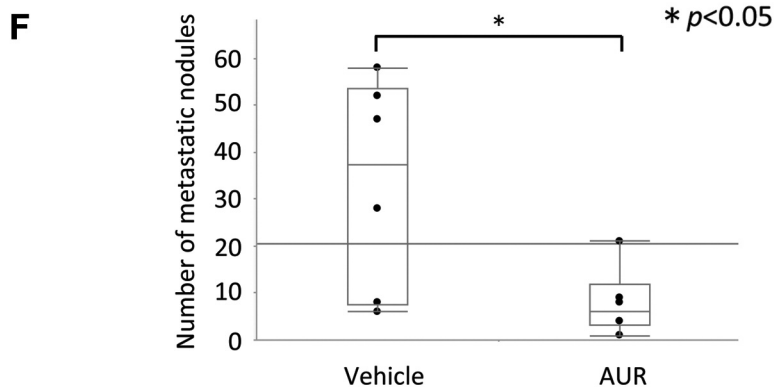
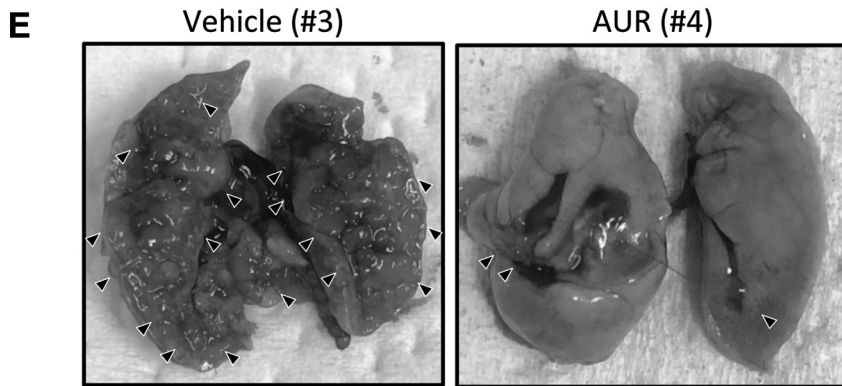
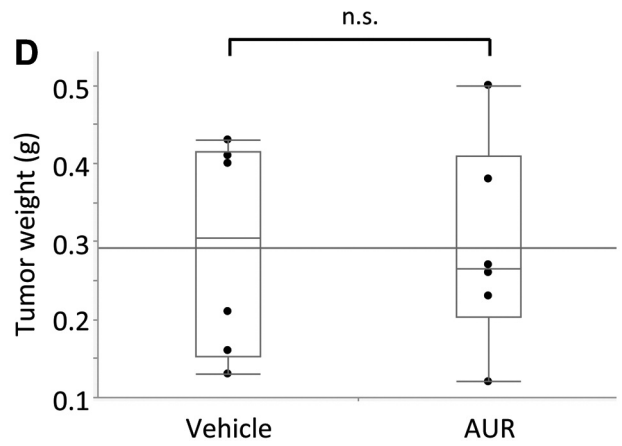
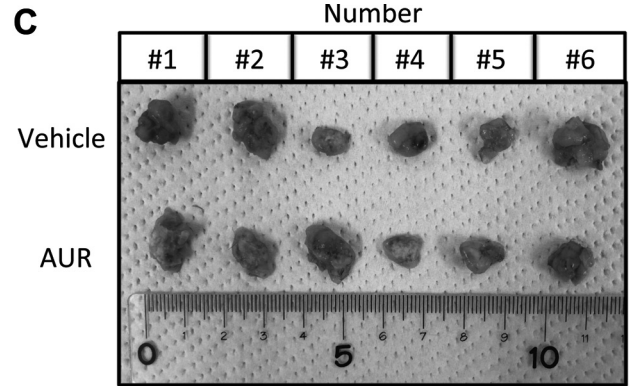
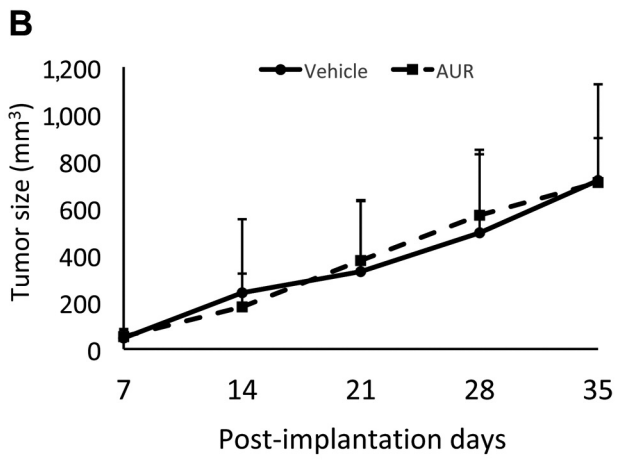
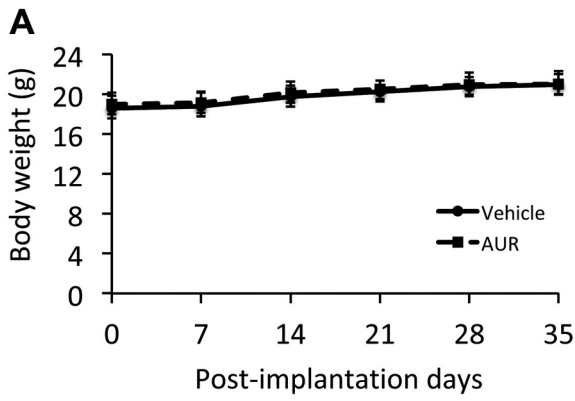


Figure 5. AUR suppressed the migration of OS cells. (A) AUR (1  $\mu$ M) reduced the migration of LM8 cells in a wound healing assay in a time-dependent manner at 12 and 24 h. (B) Significant differences were found between DMSO and AUR treatments in the calculated healed wound area; \* $p$ <0.05 (n=3). AUR: Auranofin; DMSO: dimethyl sulphoxide.

wound healing assays. AUR treatment attenuated the time-dependent migration of LM8 cells (Figure 5A). There were significant differences between DMSO and AUR treatments in the calculated healed wound area (Figure 5B).

*AUR inhibited pulmonary metastasis of OS, but not local progression.* We evaluated the effects of AUR on local progression and pulmonary metastasis of OS in a mouse



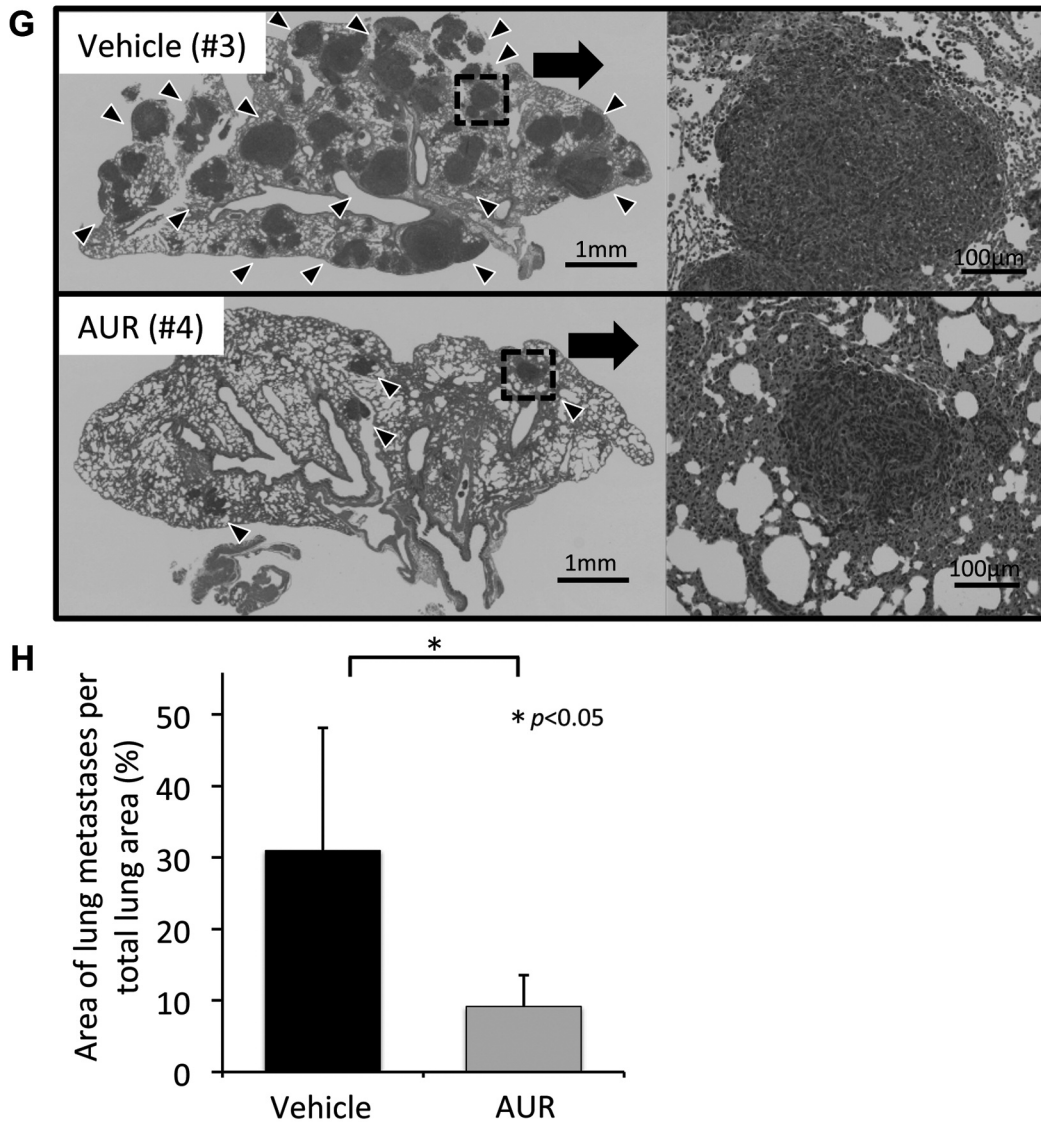


Figure 6. AUR inhibited pulmonary metastasis of OS, but not local progression. (A) There was no significant difference in body weight between mice receiving vehicle and AUR treatments during the course of the experiment. (B) AUR was not effective against local tumor progression of OS over time based on the evaluation of tumor volume. (C, D) There was no significant difference in tumor size or weight at the time of excision. (E) Photographs of mouse lungs of the vehicle and AUR groups corresponding to the tumor numbering described in Figure 6C. The local tumors of the vehicle (#3) and AUR (#4) groups were almost the same size and weight. Although the lung specimen of the vehicle (#3) group indicated numerous lung metastatic nodules, the AUR (#4) group showed only a few nodules (arrow head). (F) There were significant differences in the number of lung metastatic nodules between the vehicle and AUR groups. (G) Microscopic evaluation showed that lung metastasis was suppressed in the AUR group compared to that in the vehicle group. (H) Quantitative evaluation of the lung metastasis area showed that AUR significantly reduced pulmonary metastasis of OS compared to that in the vehicle group. \* $p < 0.05$ . OS: Osteosarcoma; AUR: auranofin.

model. There was no significant difference in body weight between the vehicle and AUR group during the course of the study (Figure 6A). In contrast to our expectation, AUR was not effective against local OS tumor progression over time based on evaluation of tumor volume (Figure 6B). Furthermore, there was no significant difference in tumor

size or weight at the time of excision (Figure 6C and D). However, the gross number of lung metastatic nodules of OS in the AUR group was significantly reduced (Figure 6E and F). Pathological and quantitative evaluation showed that AUR significantly reduced pulmonary metastasis of OS (Figure 6G and H).

## Discussion

The redox system, including TXNs and TXNRDs, is related to the local progression and metastasis of several cancers (10, 11). An oxidation-reduction imbalance induces oxidative stress, which leads to the death of cancer cells. Many anticancer drugs exert their effects by inducing oxidative stress in cancer cells (12). Samaranayake *et al.* reported that TXN-1 protects cells against androgen receptor-induced redox vulnerability in castration-resistant prostate cancer, suggesting that TXN-1 inhibitors such as PX-12 represent therapeutic agents for treating progressive prostate cancer (13). Furthermore, PX-12 induces mitochondria-mediated apoptosis in acute lymphoblastic leukemia cells (14). In contrast, the TXNRD inhibitor AUR used in the current study inhibits the proliferation of lung cancer cells *via* necrosis and caspase-dependent apoptosis (15). Topkas *et al.* reported that TXNRD2 may represent a novel therapeutic target that can reduce the development of pulmonary metastases in patients with OS (16). Furthermore, AUR has been shown to improve the overall survival when combined with standard chemotherapy in a pilot study on OS dogs (17). However, to the best of our knowledge, no studies have evaluated the efficacy of AUR alone without other anticancer drugs for suppressing local progression and pulmonary metastasis of OS.

In the current study, we performed bioinformatics analysis and found that TXNRD-2 may function as a negative prognostic factor for metastasis and overall survival in patients with OS. *In vitro* assays showed that AUR induced apoptosis *via* the oxidative stress-MAPK-Caspase 3 pathway and further suppressed the migration of OS cells. Furthermore, AUR alone significantly inhibited pulmonary metastasis of OS, but not the local progression *in vivo*.

We found that AUR alone was not effective in suppressing local progression of OS in a murine model, despite inducing *in vitro* apoptosis of OS cells. In similar *in vivo* studies, AUR alone has been found to be ineffective in treating various cancers and is being evaluated in combination with other chemotherapeutic or oxidative stress-inducing agents (18-20). Doxorubicin, a key drug used in the chemotherapy of OS, has also been shown to induce oxidative stress (21). The evaluation of the combination of AUR and doxorubicin for suppressing local progression of OS should be considered. AUR alone markedly suppressed pulmonary metastasis of OS in this assay. The prognosis for patients with pulmonary metastases of OS is very poor, with five-year survival rates as low as 10-20% (22). Local OS is removed *via* wide excision, and postoperative anticancer drugs are then administered in an attempt to suppress pulmonary metastasis (1). Consequently, the postoperative control of pulmonary metastasis is directly related to the prognosis. Therefore, it is of great importance that AUR was found to control lung metastasis of OS. Furthermore, it is important to note that AUR was developed more than 30 years ago as a safe oral therapy for rheumatoid arthritis and is approved by the FDA.

The current study has a few limitations. First, we could not elucidate the detailed mechanism *via* which AUR suppressed the pulmonary metastasis of OS. Metalloproteinases have been found to be overexpressed in OS cells, which help OS cells survive, grow, and metastasize to distant areas, mainly to the lungs (23). Li *et al.* reported that parathyroid hormone receptor 1 is essential for the proliferation and metastasis of OS (24). The mechanism of pulmonary metastasis of OS has not been fully elucidated; however, further detailed investigation of the mechanism of metastasis associated with AUR treatment is required. Second, only murine cell lines and mouse models were tested in the current study; therefore, it is necessary to use patient-derived xenografts in future studies. Finally, to inhibit local progression of OS, drugs that can be used in combination with AUR need to be investigated.

## Conclusion

The current study found that AUR significantly inhibited pulmonary metastasis of OS, but not its local progression *in vivo*. Future studies should clarify the mechanism of OS metastasis and identify drugs that are effective in combination with AUR in suppressing local progression of OS.

## Conflicts of Interest

The Authors have no conflicts of interest directly relevant to the content of this article.

## Authors' Contributions

H.K designed and performed experiments, analyzed data and wrote the article; O.S, T.I, H.K, Y.H, T.T, S.O and T.Y provided technical support and conceptual advice.

## Acknowledgements

This work was supported by JSPS KAKENHI grants (19K16760), Cancer Research Funds for Patients and Family, Foundation for Promotion of Cancer Research in Japan, Funds for Inohana Shougakukai, Funds for Children's Cancer Association of Japan, Funds for Gold Ribbon Network and Kawano Masanori Memorial Public Interest Incorporated Foundation for Promotion of Pediatrics.

## References

- 1 Kinoshita H, Yonemoto T, Kamoda H, Hagiwara Y, Tsukanishi T, Inoue M, Terakawa F, Ohtori S and Ishii T: Effectiveness of salvage knee rotationplasty on sarcoma around the knee in adolescents and young adults. *Anticancer Res* 41(2): 1041-1046, 2021. PMID: 33517313. DOI: 10.21873/anticancer.14860
- 2 Yang M, Zhang W, Yu X, Wang F, Li Y, Zhang Y and Yang Y: Helenalin facilitates reactive oxygen species-mediated apoptosis and cell cycle arrest by targeting thioredoxin reductase-1 in human prostate cancer cells. *Med Sci Monit* 27: e930083, 2021. PMID: 34125740. DOI: 10.12659/MSM.930083

- 3 Kinoshita H, Orita S, Inage K, Yamauchi K, Abe K, Inoue M, Norimoto M, Umimura T, Eguchi Y, Fujimoto K, Shiga Y, Kanamoto H, Aoki Y, Furuya T, Suzuki M, Akazawa T, Takahashi K and Ohtori S: Skeletal muscle cell oxidative stress as a possible therapeutic target in a denervation-induced experimental sarcopenic model. *Spine (Phila Pa 1976)* *44*(8): E446-E455, 2019. PMID: 30299418. DOI: 10.1097/BRS.0000000000002891
- 4 Al-Khayal K, Vaali-Mohammed MA, Elwatidy M, Bin Traiki T, Al-Obeed O, Azam M, Khan Z, Abdulla M and Ahmad R: A novel coordination complex of platinum (PT) induces cell death in colorectal cancer by altering redox balance and modulating MAPK pathway. *BMC Cancer* *20*(1): 685, 2020. PMID: 32703189. DOI: 10.1186/s12885-020-07165-w
- 5 Scalcon V, Bindoli A and Rigobello MP: Significance of the mitochondrial thioredoxin reductase in cancer cells: An update on role, targets and inhibitors. *Free Radic Biol Med* *127*: 62-79, 2018. PMID: 29596885. DOI: 10.1016/j.freeradbiomed.2018.03.043
- 6 El Feky SE, Ghany Megahed MA, Abd El Moneim NA, Zaher ER, Khamis SA and Ali LMA: Cytotoxic, chemosensitizing and radiosensitizing effects of curcumin based on thioredoxin system inhibition in breast cancer cells: 2D vs. 3D cell culture system. *Exp Ther Med* *21*(5): 506, 2021. PMID: 33791015. DOI: 10.3892/etm.2021.9937
- 7 Freire Boulosa L, Van Loenhout J, Flieswasser T, De Waele J, Hermans C, Lambrechts H, Cuyper B, Laukens K, Bartholomeus E, Siozopoulou V, De Vos WH, Peeters M, Smits ELJ and Deben C: Auranofin reveals therapeutic anticancer potential by triggering distinct molecular cell death mechanisms and innate immunity in mutant p53 non-small cell lung cancer. *Redox Biol* *42*: 101949, 2021. PMID: 33812801. DOI: 10.1016/j.redox.2021.101949
- 8 Wang J, Wang J, Lopez E, Guo H, Zhang H, Liu Y, Chen Z, Huang S, Zhou S, Leeming A, Zhang RJ, Jung D, Shi H, Grundman H, Doakes D, Cui K, Jiang C, Ahmed M, Nomie K, Fang B, Wang M, Yao Y and Zhang L: Repurposing auranofin to treat TP53-mutated or PTEN-deleted refractory B-cell lymphoma. *Blood Cancer J* *9*(12): 95, 2019. PMID: 31780660. DOI: 10.1038/s41408-019-0259-8
- 9 Sannella AR, Casini A, Gabbiani C, Messori L, Bilia AR, Vincieri FF, Majori G and Severini C: New uses for old drugs. Auranofin, a clinically established antiarthritic metallodrug, exhibits potent antimalarial effects *in vitro*: Mechanistic and pharmacological implications. *FEBS Lett* *582*(6): 844-847, 2008. PMID: 18294965. DOI: 10.1016/j.febslet.2008.02.028
- 10 Qayyum N, Haseeb M, Kim MS and Choi S: Role of thioredoxin-interacting protein in diseases and its therapeutic outlook. *Int J Mol Sci* *22*(5): 2754, 2021. PMID: 33803178. DOI: 10.3390/ijms22052754
- 11 Zhang J, Duan D, Osama A and Fang J: Natural molecules targeting thioredoxin system and their therapeutic potential. *Antioxid Redox Signal* *34*(14): 1083-1107, 2021. PMID: 33115246. DOI: 10.1089/ars.2020.8213
- 12 Lincoln DT, Ali Emadi EM, Tonissen KF and Clarke FM: The thioredoxin-thioredoxin reductase system: over-expression in human cancer. *Anticancer Res* *23*(3B): 2425-2433, 2003. PMID: 12894524.
- 13 Samaranayake GJ, Troccoli CI, Huynh M, Lyles RDZ, Kage K, Win A, Lakshmanan V, Kwon D, Ban Y, Chen SX, Zarco ER, Jorda M, Burnstein KL and Rai P: Thioredoxin-I protects against androgen receptor-induced redox vulnerability in castration-resistant prostate cancer. *Nat Commun* *8*(1): 1204, 2017. PMID: 29089489. DOI: 10.1038/s41467-017-01269-x
- 14 Ehrenfeld V and Fulda S: Thioredoxin inhibitor PX-12 induces mitochondria-mediated apoptosis in acute lymphoblastic leukemia cells. *Biol Chem* *401*(2): 273-283, 2020. PMID: 31352431. DOI: 10.1515/hsz-2019-0160
- 15 Cui XY, Park SH and Park WH: Auranofin inhibits the proliferation of lung cancer cells *via* necrosis and caspase-dependent apoptosis. *Oncol Rep* *44*(6): 2715-2724, 2020. PMID: 33125149. DOI: 10.3892/or.2020.7818
- 16 Topkas E, Cai N, Cumming A, Hazar-Rethinam M, Gannon OM, Burgess M, Saunders NA and Endo-Munoz L: Auranofin is a potent suppressor of osteosarcoma metastasis. *Oncotarget* *7*(1): 831-844, 2016. PMID: 26573231. DOI: 10.18632/oncotarget.5704
- 17 Endo-Munoz L, Bennett TC, Topkas E, Wu SY, Thamm DH, Brockley L, Cooper M, Sommerville S, Thomson M, O'Connell K, Lane A, Bird G, Peaston A, Matigian N, Straw RC and Saunders NA: Auranofin improves overall survival when combined with standard of care in a pilot study involving dogs with osteosarcoma. *Vet Comp Oncol* *18*(2): 206-213, 2020. PMID: 31441983. DOI: 10.1111/vco.12533
- 18 Joo MK, Shin S, Ye DJ, An HG, Kwon TU, Baek HS, Kwon YJ and Chun YJ: Combined treatment with auranofin and trametinib induces synergistic apoptosis in breast cancer cells. *J Toxicol Environ Health A* *84*(2): 84-94, 2021. PMID: 33103613. DOI: 10.1080/15287394.2020.1835762
- 19 Hwangbo H, Kim SY, Lee H, Park SH, Hong SH, Park C, Kim GY, Leem SH, Hyun JW, Cheong J and Choi YH: Auranofin enhances sulforaphane-mediated apoptosis in hepatocellular carcinoma Hep3B cells through inactivation of the PI3K/Akt signaling pathway. *Biomol Ther (Seoul)* *28*(5): 443-455, 2020. PMID: 32856616. DOI: 10.4062/biomolther.2020.122
- 20 Ryu YS, Shin S, An HG, Kwon TU, Baek HS, Kwon YJ and Chun YJ: Synergistic induction of apoptosis by the combination of an Axl inhibitor and auranofin in human breast cancer cells. *Biomol Ther (Seoul)* *28*(5): 473-481, 2020. PMID: 32536618. DOI: 10.4062/biomolther.2020.051
- 21 Zhang S and Guo W:  $\beta$ -elemene enhances the sensitivity of osteosarcoma cells to doxorubicin *via* downregulation of peroxiredoxin-1. *Onco Targets Ther* *14*: 3599-3609, 2021. PMID: 34113126. DOI: 10.2147/OTT.S303152
- 22 Jiang Y, Li F, Gao B, Ma M, Chen M, Wu Y, Zhang W, Sun Y, Liu S and Shen H: KDM6B-mediated histone demethylation of LDHA promotes lung metastasis of osteosarcoma. *Theranostics* *11*(8): 3868-3881, 2021. PMID: 33664867. DOI: 10.7150/thno.53347
- 23 Hadjimichael AC, Foukas AF, Savvidou OD, Mavrogenis AF, Psyrris AK and Papagelopoulos PJ: The anti-neoplastic effect of doxycycline in osteosarcoma as a metalloproteinase (MMP) inhibitor: a systematic review. *Clin Sarcoma Res* *10*: 7, 2020. PMID: 32377334. DOI: 10.1186/s13569-020-00128-6
- 24 Li S, Pei Y, Wang W, Liu F, Zheng K and Zhang X: Quercetin suppresses the proliferation and metastasis of metastatic osteosarcoma cells by inhibiting parathyroid hormone receptor 1. *Biomed Pharmacother* *114*: 108839, 2019. PMID: 30978523. DOI: 10.1016/j.biopha.2019.108839

Received June 29, 2021

Revised August 30, 2021

Accepted August 31, 2021